



## Time-periodic Electroosmotic Flow of Non-newtonian Fluids in Microchannels

A. Jabari Moghadam\*, P. Akbarzadeh

Department of Mechanical Engineering, Shahrood University of Technology, Shahrood, Iran

## P A P E R I N F O

## Paper history:

Received 12 December 2015

Received in revised form 02 January 2016

Accepted 03 May 2016

## Keywords:

Microfluidics

AC Electroosmotic Flow

Shear-thinning and Shear-thickening Fluids

Circular Microchannel

Frequency

## A B S T R A C T

The alternating current electroosmotic flow of a non-Newtonian power-law fluid is studied in a circular microchannel. A numerical method is employed to solve the non-linear Poisson-Boltzmann and the momentum equations. The main parameters which affect the flow field are the flow behavior index, the dimensionless zeta potential and the dimensionless frequency. At very low dimensionless frequencies (slow oscillatory motion, small channel size, or large effective viscosity), the plug-like velocity profiles similar to steady-state electroosmotic flow are observed at nearly all times. At very high dimensionless frequencies, the flow is shown to be restricted to a thin region near the channel wall, while the bulk fluid remains essentially stationary. Velocity distributions of pseudoplastics and dilatants may be widened at low values of the dimensionless frequency depending on the dimensionless zeta potential; at high dimensionless frequencies, however, both fluids represent enhanced velocity magnitudes with the dimensionless zeta potential. In the case of high shear rate and/or suddenly-started flows, pseudoplastics tend to produce higher velocities than dilatants. These two kinds of fluids may produce same velocity profiles relying on the value of the dimensionless zeta potential as well as the ratio of their flow behavior indexes.

doi: 10.5829/idosi.ije.2016.29.05b.15

## Nomenclature

$d$	auxiliary variable = $dV / dR$	$z$	axial coordinate [m]
$D$	auxiliary variable = $d^3V / dR^2$	$Z$	dimensionless potential at the wall
$e$	electron charge [C]	$\aleph$	Valence of ionic species
$E$	electrical field strength along axial direction [V/m]	<b>Greek symbols</b>	
$G_i^m$	auxiliary variable = $d ( dV / dR ) / dR$	$\chi$	the electro-kinetic radius
$h$	numerical step for radius direction	$\varepsilon$	electric permittivity of solution [F/m]
$k_B$	Boltzmann constant [J/K]	$\kappa$	Debye-Hückel parameter [m <sup>-1</sup> ]
$K$	flow consistency index	$\theta$	dimensionless time
$n$	flow behavior index	$\rho$	fluid density [kg/m <sup>3</sup> ]
$n_0$	bulk ion concentration [m <sup>-3</sup> ]	$\rho_e$	net volume charge density [C m <sup>-3</sup> ]
$r$	radial coordinate [m]	$\tau$	time scale
$\mathcal{R}$	radius of the micro-channel [m]	$U$	numerical step for time
$R$	dimensionless radial coordinate	$\omega$	frequency [s <sup>-1</sup> ]
$t$	time [s]	$\Omega$	dimensionless frequency
$T$	absolute temperature [K]	$\Psi$	electrical potential [V]
$u$	auxiliary variable = $d\Psi / dR$	$\psi$	dimensionless electrical potential
$V$	dimensionless axial velocity	$\zeta$	zeta potential [V]
$V_z$	axial velocity [m/s]	<b>index</b>	
$V_{hs}$	the Helmholtz-Smoluchowski velocity	$i, m$	

\*Corresponding Author's Email: alijabari@shahroodut.ac.ir (A. Jabari Moghadam)

## 1. INTRODUCTION

Microfluidics is a technological field that deals with the flow and handling of fluids in micro-sized systems influenced by external electric forces. This field is mainly driven by technological applications; the vision is to develop entire bio/chemical laboratories on the surface of silicon or polymer chips. Microfluidic devices are significantly applied in micro-electro-mechanical systems (MEMS) and bio-sensor areas, such as lab-on-a-chip (LOC). Miniaturized fluidic systems (consisting of micro-ducts, valves, pumps and various other injection systems) can be utilized in medical, pharmaceutical and defense applications, for instance in drug delivery, DNA analysis and sequencing and biological/chemical agent detection sensors on micro-chips. The main advantages of these emerging microfluidic technologies are their low-cost, light-weight and small-size. Electroosmosis is defined as the motion of ionized liquid relative to the stationary charged surface by an applied electric field. A dilute solution in contact to a surface with trapped surface charge experiences redistribution of its ions leading to formation of electric double layer (EDL). The electroosmotic flow (EOF) is created by applying an effective electric field in the streamwise direction. For a wide class of fluids and solution, the so-called non-Newtonian fluids, the assumption of constant viscosity does not apply. If a liquid, such as polymer solutions or blood, contains large deformable molecules or particles, these can be stretched out at an increased shear stress, which then can lead to a decrease in viscosity. In other fluids containing small, strongly interacting particles, the inter-particle interaction can impede the flow at an increased shear stress, which then can lead to an increased viscosity. These two opposite effects are denoted shear-thinning and shear-thickening, respectively; they form a central topic in the field of rheology [1].

Various studies on EOF in microchannels have been conducted under different geometric and physical conditions. Among them, Ajdari [2] reported the effect of inhomogeneously charged surfaces on electroosmosis. Bhattacharyya and Nayak [3] studied effects of geometric and surface potential heterogeneity of EOF in micro/nano channels. They observed that these effects lead to a formation of vortex adjacent to the potential patch as well as an induced pressure gradient. Arulanandam and Li [4] studied the liquid movement in a rectangular micro-channel by electroosmotic pumping. The electrokinetic and hydrodynamic transport effects under the application of combined pressure and DC electric fields were examined by Bhattacharyya and Bera [5] for different values of EDL thickness and channel patch potential. Kang et al. [6] solved the electroosmotic flow in a cylindrical channel

for the sine waveform. Cho et al. [7] presented a numerical solution of time-periodic EOF in a microchannel with a complex-wavy surface. As an alternative to traditional DC electroosmosis, a series of novel techniques have been developed to generate bulk flow using AC fields. Experimental and analytical studies were reported on the flow induced by non-uniform AC electric fields in electrolytes [8, 9]. Using similar patterns, both Brown et al. [10] and Studer et al. [11] presented microfluidic devices that incorporated arrays of non-uniformly sized embedded electrodes which, when subject to an AC field, can generate a bulk fluid motion. Alternating current EOF through microchannels was conducted by some other researchers [12, 13]; the latter presented analogies to Stokes' second problem. Also, Moghadam [14-16] presented analytical solutions, via Green's functions formulation, for AC electroosmotic flow in circular and annular microchannels.

A theoretical investigation of electroosmotic mobility of non-Newtonian fluids was reported by Zhao and Yang [17]. Electroosmotic flow of power-law fluids in a circular microchannel was studied by Zhao and Yang [18], and some analytical expressions were obtained for special cases. Tang et al. [19] reported a numerical study of EOF in microchannels considering the non-Newtonian behavior. Mondal and De [20] studied mass transport together with EOF of a power-law fluid in a porous microtube.

The technological demands on microfluidic systems require a better understanding of the micro-scale fluidic transport phenomena. To the authors' knowledge, time-periodic EOF of non-Newtonian fluids in microdevices has not been considered in the literature. In this research, a numerical analysis is performed on AC electroosmotic flows of non-Newtonian incompressible fluids (based on the Ostwald-de Waele power-law model) in microchannels. Effects of governing parameters on the flow characteristics of pseudoplastics (shear-thinning fluids) and dilatants (shear-thickening fluids) are also investigated.

## 2. Model Description

At equilibrium, solid surfaces have a net surface charge density, because of ionization and adsorption processes. The immobile charge on the surface is balanced at equilibrium by a mobile diffuse volumetric charge density. Equivalently, ions with like charge to the wall (coions) are repelled from the region near the wall, whereas ions with opposite charge to the wall (counterions) are attracted to the region near the wall. In the current study, the fully-developed pure EOF of a non-Newtonian power-law fluid is considered in a circular microchannel. It is assumed that the fluid is

composed of one symmetric electrolyte, the channel wall is uniformly charged, and an external periodic electric field is applied along the microchannel. The electric potential distribution in the EDL region and the velocity distribution in the cross-sectional area of the microchannel are governed by the following non-linear Poisson-Boltzmann and modified Cauchy momentum equations, respectively [1, 21, 22]:

$$\frac{1}{r} \frac{d}{dr} \left( r \frac{d\psi}{dr} \right) = \frac{2\aleph e n_0}{\varepsilon} \sinh \left( \frac{\aleph e}{k_B T} \psi \right) \quad (1)$$

$$\rho \frac{\partial V_z}{\partial t} = \frac{K}{r} \frac{\partial}{\partial r} \left[ r \left( -\frac{\partial V_z}{\partial r} \right)^n \right] + 2\aleph e n_0 \sinh \left( \frac{\aleph e}{k_B T} \psi \right) E(\omega t) \quad (2)$$

where,  $V_z$  is the only non-zero velocity component along the channel,  $\rho$  and  $\mu$  are density and viscosity of liquid, respectively, and  $E(\omega t) = E_z F(\omega t)$  is a general time-periodic function with a frequency  $\omega = 2\pi f$  that describes the applied electric field strength.  $E_z$  is a constant and  $F(\omega t)$  is the oscillatory function of unit magnitude. The quantities  $K$  and  $n$  are the flow consistency index and the flow behavior index, respectively.

The above equations are subjected to the following boundary conditions:

$$\begin{cases} r=0 & : \frac{d\psi}{dr} = 0 \\ r=\aleph & : \psi = \zeta \end{cases} \quad (3)$$

$$\begin{cases} r=0 & : \frac{\partial V_z}{\partial r} = 0 \\ r=\aleph & : V_z = 0 \end{cases} \quad (4)$$

where,  $\aleph$  and  $\zeta$  are the channel radius and the wall zeta potential, respectively. Consider the following dimensionless variables:

$$R = \frac{r}{\aleph}, \quad \Psi = \frac{\aleph e}{k_B T} \psi, \quad V = \frac{V_z}{V_{HS}} \quad (5)$$

$$\theta = \frac{t}{\tau}, \quad \Omega = \omega \tau$$

in which, the Helmholtz-Smoluchowski velocity  $V_{HS}$  and the time scale  $\tau$  are given by:

$$V_{HS} = n \kappa^n \left( \frac{\varepsilon k_B T E_z}{K \aleph e} \right)^{1/n} \quad (6)$$

$$\tau = \frac{\rho \aleph^{1+n}}{2\aleph e n_0 E_z} \frac{\kappa^n}{n^n} V_{HS} \quad (7)$$

$\kappa$  is the Debye-Huckel parameter defined as follows:

$$\kappa = \left( \frac{2\aleph^2 e^2 n_0}{\varepsilon k_B T} \right)^{1/2} \quad (8)$$

Substituting the non-dimensional variables (5) into Equations (1) and (2), we find:

$$\frac{1}{R} \frac{d}{dR} \left( R \frac{d\Psi}{dR} \right) = \chi^2 \sinh(\Psi) \quad (9)$$

$$\frac{\partial V}{\partial \theta} = \frac{-1}{R} \frac{\partial}{\partial R} \left[ R \left( -\frac{\partial V}{\partial R} \right)^n \right] + \frac{\chi^{1+n}}{n^n} \sinh(\Psi) F(\Omega \theta) \quad (10)$$

in which,  $\chi = \kappa \aleph$  is the electrokinetic radius. The dimensionless boundary conditions are:

$$\begin{cases} R=0 & : \frac{d\Psi}{dR} = 0 \\ R=1 & : \Psi = Z \end{cases} \quad (11)$$

$$\begin{cases} R=0 & : \frac{\partial V}{\partial R} = 0 \\ R=1 & : V = 0 \end{cases} \quad (12)$$

### 3. Solution Procedure

In order to obtain the value of electrical potential variable ( $\Psi$ ), the non-linear 2<sup>nd</sup>-order boundary value problem of Relation (9) is replaced by two 1<sup>st</sup>-ODEs as follows:

$$\begin{cases} u = \Psi' \\ R u' + u - R \chi^2 \sinh \Psi = 0 \end{cases} \quad (13)$$

By using central difference method and discretizing Equation (13) around space grid-point  $i-1/2$ , the following relations are achieved:

$$\frac{u_{i-1} + u_i}{2} = \frac{\Psi_i - \Psi_{i-1}}{h}$$

$$(R_{i-1} + R_i) \left( \frac{u_i - u_{i-1}}{h} \right) + (u_{i-1} + u_i) \quad (14)$$

$$-(R_{i-1} + R_i) \chi^2 \sinh \left( \frac{\Psi_{i-1} + \Psi_i}{2} \right) = 0$$

where,  $h = \Delta R$  is the step for radial direction. Finally, Equations (14) and (11) are solved using Newton's method (i.e.,  $\Psi_i^{k+1} = \Psi_i^k + \Delta \Psi_i^k$  and  $u_i^{k+1} = u_i^k + \Delta u_i^k$ , where  $k$  is the iterative index) and a block tridiagonal matrix solver (such as Tomas Algorithm) [23]. After calculating  $\Psi$ , Equation (10) is solved by a discretized version of it, using the forward difference

approximation in term of time and the central difference approach in the space direction both 1<sup>st</sup>-order derivative and 2<sup>nd</sup>-order derivative as follows:

$$V_i^{m+1} = V_i^m + \nu \left( d_i^m / R_i + D_i^m \right) |d|^{n-1} + \nu D_i^m G_i^m + \nu \frac{\chi^{1+n}}{n} (\sinh \Psi_i) F(\Omega \theta^m) \tag{15}$$

where,  $\nu = \Delta\theta$  is the time-step,  $m$  is the index for march of time,  $\theta^m = m\nu$  is the spending time,  $D_i^m = (V_{i+1}^m - 2V_i^m + V_{i-1}^m) / h^2$ ,  $d_i^m = (V_{i+1}^m - V_{i-1}^m) / (2h)$ , and  $G_i^m = |(V_{i+1}^m - V_i^m) / h|^{n-1} - |(V_i^m - V_{i-1}^m) / h|^{n-1}$ .

**4. Results and Discussion**

Investigations into the AC electroosmotic flow of power-law fluids in microchannels reveal that the dimensionless potential distribution is a function of the electrokinetic radius ( $\chi$ ) and the non-dimensional wall potential ( $Z$ ); the dimensionless velocity profile depends on  $\chi$  and  $Z$  as well as on the flow behavior index ( $n$ ), the dimensionless frequency ( $\Omega$ ), and time ( $\theta$ ). The periodic function of unit magnitude is selected as  $F(\Omega\theta) = \sin(\Omega\theta)$ . An EOF micropump with  $\chi = 500$  and  $Z = 0.5$  is equivalent to  $\kappa = 2 \times 10^7 m^{-1}$  in a  $50 \mu m$  channel with a uniform surface potential of  $\zeta = 12.5 mV$ . The key governing parameter in our formulation is  $\Omega$  which can be interpreted as the ratio of the diffusion time scale,  $t_D = \tau = \rho \mathfrak{R}^{1+n} / \mu_{eff}$ , to the period of the applied electric field,  $t_E = 1/\omega$ .  $\mu_{eff}$  is defined as the fluid effective viscosity.

Figure 1 shows the dimensionless potential distribution as a function of various  $\chi$  and  $Z$ . As the value of  $\chi$  is increased (by increasing the bulk ion concentration in the liquid), the electric double layer is confined to the channel wall, resulting in sharp variations in the electric potential. The electric potential at the middle of the channel is practically zero. A comparison of the current numerical solution to the exact solution [14] is represented in Figure 2 for different values of the governing parameters. It is obviously found that the results of each set are in great agreement.

Figure 3 depicts the dimensionless velocity profiles in one period of the sinusoidal waveform for  $Z = 0.5$ ,  $\chi = 300$ , and different values of  $n$  and  $\Omega$ .

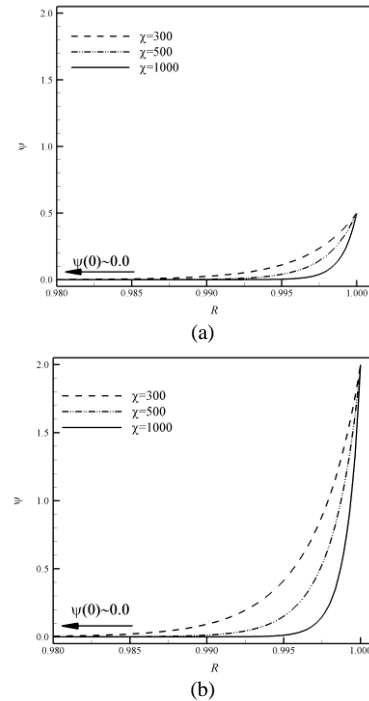


**Figure 1.** Dimensionless potential distribution for various values of  $\chi$  and (a)  $Z = 0.5$  and (b)  $Z = 2$

As the value of  $\Omega$  is increased, the amplitude of change in the middle-area velocity is decreased; for sufficiently high values of  $\Omega$ , the bulk fluid is not moving, while the fluid within the EDL oscillates rapidly.

The steady-state time-periodic motion of the fluid influenced by a very low frequency (e.g.  $\Omega = 0.3$ ) is illustrated in Figure 3a (and also Figure 4a), that demonstrates the plug-like velocity distributions at nearly all times. The influence of the flow behavior index on the flow field (for  $Z = 0.5$ ) is to broaden the velocity profile, especially at the near-wall regions where peaks are observed. A reverse behavior is shown for  $Z = 2$  in Figure 4.

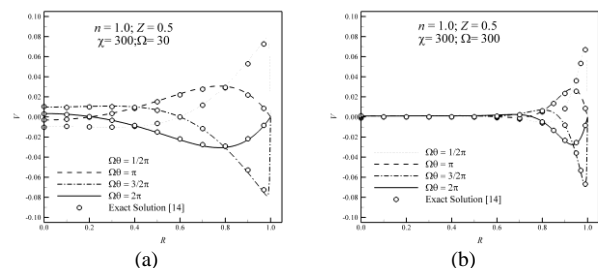


**Figure 2.** Steady-state time-periodic non-dimensional velocity distribution of Newtonian fluids for various values of  $Z, \Omega, \chi$

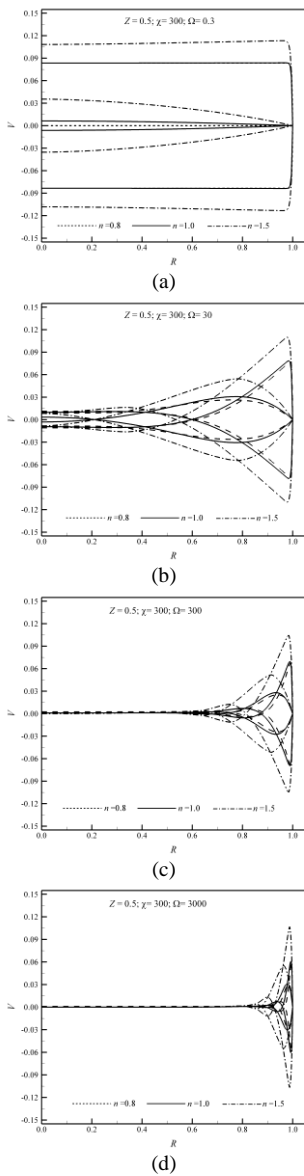


**Figure 3.** Steady-state time-periodic dimensionless velocity profiles for one period ( $\Omega\theta = \pi/2, \pi, 3\pi/2, 2\pi$ ) of the sinusoidal waveform for  $Z = 0.5$

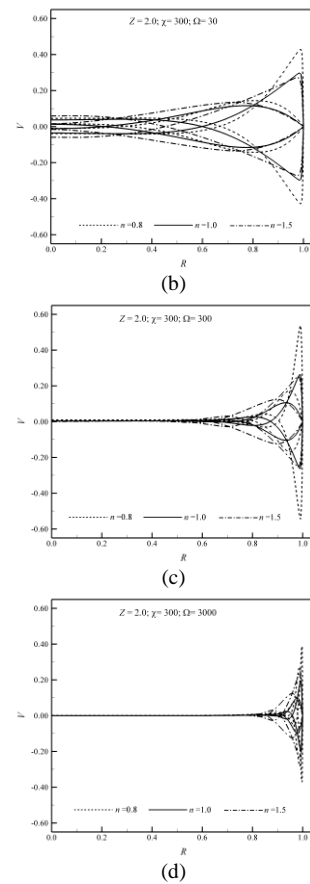
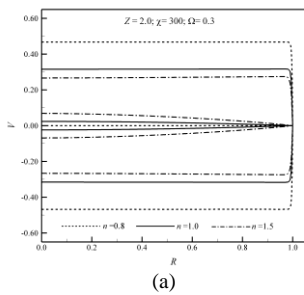


**Figure 4.** Steady-state time-periodic dimensionless velocity profiles for one period ( $\Omega\theta = \pi/2, \pi, 3\pi/2, 2\pi$ ) of the sinusoidal waveform for  $Z = 2$

A comparison of Figures 3 and 4 (for instant, Figure 3a and Figure 4a) reveals that higher values of the dimensionless zeta potential lead to enhanced velocity distribution for  $n < 1$ ; since in this case, effective viscosity decreases with increasing shear rate, and the flow field is enlarged.

A comprehensive study of the effect of non-dimensional zeta potential on the velocity profiles is illustrated in Figure 5. As discussed in Figures 3 and 4, for small values of  $Z$  (less than one), an increase in  $n$  results in an increase in  $V$  near the wall as well as a decrease in  $v$  near the centerline. As the value of  $Z$  rises above one, the foregoing trend is reversed. In the case of  $Z=1$  (Figure 5c), the maximum values of velocity profiles of non-Newtonian fluids ( $n \neq 1$ ) coincide roughly. In fact, there is one special  $Z$  in which the velocity profiles of shear-thinning and shear-thickening fluids coincide exactly.

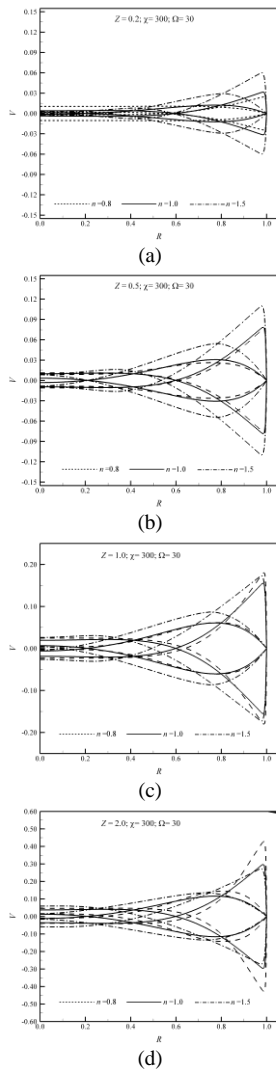


**Figure 5.** Effect of non-dimensional zeta potential on dimensionless velocity profiles

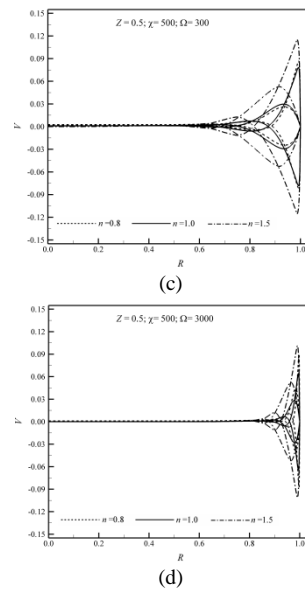
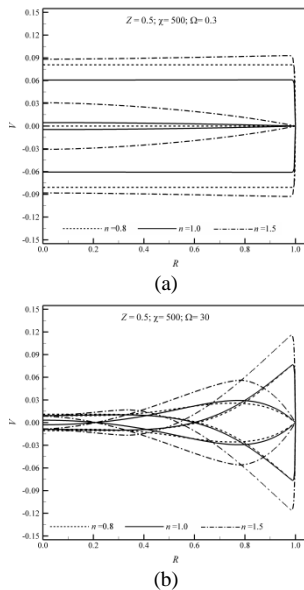


**Figure 6.** Steady-state time-periodic dimensionless velocity profiles for one period ( $\Omega\theta = \pi/2, \pi, 3\pi/2, 2\pi$ ) of the sinusoidal waveform for  $Z = 0.5$  and  $\chi = 500$

The steady-state time-periodic non-dimensional velocity profiles for  $Z = 0.5$ ,  $\chi = 500$  and different values of  $n$  and  $\Omega$  are shown in Figure 6. A comparison of Figures 3a and 6a proves that the effect of  $\chi$  is to reduce the velocity for  $n \geq 1$ . Actually higher values of the electrokinetic radius correspond to smaller regions influenced by the electric double layer; hence, for very slow oscillating motion, shear-thinning fluids are not mainly affected by the electroviscous effects. For intermediate to high values of the dimensionless frequency, compared with Figure 3, it is clear that an increase in  $\kappa$  or a decrease in the Debye length leads to an increase in the maximum velocity near the channel wall; the velocity magnitude at the centerline is somewhat reduced (for a fixed mass flow rate).

Figure 7 illustrates dimensionless velocity profiles at the beginning of motion for the channel mid-point and the near-wall representative point. These two points, i.e.  $R = 0$  and  $R = 0.99$ , can be viewed as characteristics of the bulk liquid motion and the EDL liquid motion, respectively.

By comparison, the fluid within the EDL has almost instant response to the applied electric field, whereas, the bulk fluid does not (and lags behind the applied electric field by a phase shift). Additionally, the EDL fluid reaches its steady-state oscillatory situation almost immediately, while, the bulk fluid needs a finite time before the transient effects are dissipated. In general, the velocity field is proportionally scaled by  $\Omega$ ; and when this quantity is increased, the phase shift for both the EDL and the bulk fluid velocities is increased.

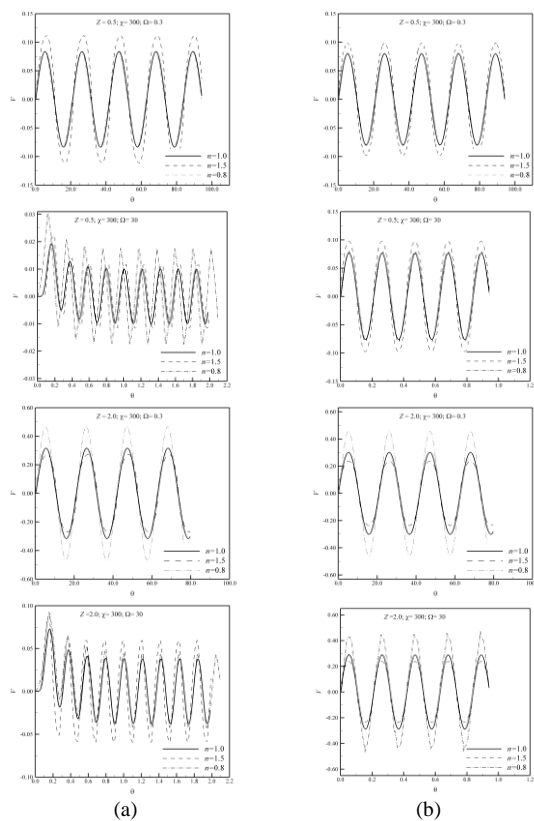


**Figure 7.** Transient stage non-dimensional velocity of (a) the channel midpoint and (b) the EDL representative point ( $R = 0.99$ ) for impulsively started flows

When  $\Omega < 1$ , on the other hand, the bulk fluid has sufficient time to respond to instantaneous changes in the applied electric field. Where shear rate is high (in the EDL region and/or when  $Z > 1$ ), shear-thinning fluids represent higher velocities than shear-thickening fluids.

## 5. Concluding Remarks

A parametric study has been implemented for the electroosmotic driven microchannel flows of non-Newtonian power-law fluids. To develop a physical intuition, the flow field response to excitation by the sinusoidal waveform has been investigated. The following is a summary of our conclusions:

- Increasing the bulk ion concentration in the liquid results in an increase in the electrokinetic radius or a decrease in the EDL thickness; correspondingly, the EDL potential field falls off to zero more rapidly with distance.
- The dimensionless frequency is directly proportional to the excitation frequency, density, and the channel size, and is inversely proportional to the effective viscosity.
- When momentum diffusion is faster than the oscillation period (very low dimensionless frequency), the plug-like velocity profile of steady-state EOF is observed at all times. On the other hand, when the diffusion time scale is much greater than the oscillation period (very high dimensionless frequency), fluid momentum does not have sufficient time to diffuse far into the bulk fluid; consequently, the fluid within the EDL oscillates rapidly, while the bulk fluid is not almost moving. At intermediate dimensionless frequencies, there is more time for momentum diffusion from the electric double layer; however, there is a finite time lag between when the EDL fluid moves and the bulk fluid follows it.
- As the electrokinetic radius is increased (EDL becomes thinner), the electroviscous resistance modifies the velocity distribution; it increases the maximum velocity near the wall, and simultaneously reduces the average velocity of the bulk fluid (for a fixed mass flow rate).
- The dimensionless zeta potential, which is a measure of the electric energy to the thermal energy at the surface, serves to scale the velocity magnitude. This quantity particularly affects the flow structure of non-Newtonian fluids.
- For low values of the dimensionless frequency, increasing the dimensionless zeta potential leads to narrow (broaden) velocity distribution of dilatants (pseudoplastics). Both dilatant and pseudoplastic fluids, however, represent enhanced velocity magnitudes with the dimensionless zeta potential when the dimensionless frequency is high enough; in this case, pseudoplastics have much higher velocities than dilatants.
- There is some degree of phase shift between the applied electric field and the flow response in the channel; this phase shift is significantly different in the EDL region than in the bulk flow. When the dimensionless frequency is increased, the phase shift for both the EDL and the bulk fluid velocities is increased.
- Impulsively started flows from rest are shown to exhibit transient behavior resulting in a net positive flow during the initial cycles for cases of high dimensionless frequency. As the dimensionless frequency is less than one, viscous diffusion is sufficiently fast to allow the bulk fluid to respond to instantaneous changes in the applied electric field.
- Where high shear rates exist and/or flows start suddenly, shear-thinning fluids tend to produce higher velocities than shear-thickening fluids.
- Shear-thinning and shear-thickening fluids may produce the same velocity profiles depending on the dimensionless zeta potential as well as the relative values of their flow behavior indexes.

## 6. References

1. Bruus, H., *Theoretical microfluidics*. 2008, New York: Oxford University Press.
2. Ajdari, A., "Electro-osmosis on inhomogeneously charged surfaces", *Physical Review Letters*, Vol. 75, No. 4, (1995), 755-758.
3. Bhattacharyya, S. and Nayak, A., "Combined effect of surface roughness and heterogeneity of wall potential on electroosmosis in microfluidic/nanofluidic channels", *Journal of Fluids Engineering*, Vol. 132, No. 4, (2010), 241-250.
4. Arulanandam, S. and Li, D., "Liquid transport in rectangular microchannels by electroosmotic pumping", *Colloids and Surfaces A: Physicochemical and Engineering Aspects*, Vol. 161, No. 1, (2000), 89-102.
5. Bhattacharyya, S. and Bera, S., "Nonlinear electroosmosis pressure-driven flow in a wide microchannel with patchwise surface heterogeneity", *Journal of Fluids Engineering*, Vol. 135, No. 2, (2013), 85-96.
6. Kang, Y., Yang, C. and Huang, X., "Dynamic aspects of electroosmotic flow in a cylindrical microcapillary", *International Journal of Engineering Science*, Vol. 40, No. 20, (2002), 2203-2221.
7. Cho, C.C., Chen, C.L. and Chen, C.K., "Characteristics of transient electroosmotic flow in microchannels with complex-wavy surface and periodic time-varying electric field", *Journal of Fluids Engineering*, Vol. 135, No. 2, (2013), 135-146.
8. Green, N.G., Ramos, A., Gonzalez, A., Morgan, H. and Castellanos, A., "Fluid flow induced by non-uniform ac electric fields in electrolytes on microelectrodes i: Experimental measurements", *Physical Review E*, Vol. 61, No., (2000), 4011-4018.
9. Gonzalez, A., Ramos, A., Green, N.G., Castellanos, A. and Morgan, H., "Fluid flow induced by non-uniform ac electric fields in electrolytes on microelectrodes ii: A linear double layer analysis", *Physical Review E*, Vol. 61, (2000), 4019-4028.
10. Brown, A., Smith, C. and Rennie, A., "Pumping of water with ac electric fields applied to asymmetric pairs of microelectrodes", *Physical Review E*, Vol. 63, No. 1, (2000), 287-295.
11. Studer, V., Pepin, A., Chen, Y. and Ajdari, A., "Fabrication of microfluidic devices for ac electrokinetic fluid pumping", *Microelectronic Engineering*, Vol. 61, (2002), 915-920.
12. Erickson, D. and Li, D., "Analysis of alternating current electroosmotic flows in a rectangular microchannel", *Langmuir*, Vol. 19, No. 13, (2003), 5421-5430.
13. Dutta, P. and Beskok, A., "Analytical solution of time periodic electroosmotic flows: Analogies to stokes' second problem", *Analytical Chemistry*, Vol. 73, No. 21, (2001), 5097-5102.
14. Moghadam, A.J., "An exact solution of ac electro-kinetic-driven flow in a circular micro-channel", *European Journal of Mechanics-B/Fluids*, Vol. 34, (2012), 91-96.
15. Moghadam, A.J., "Exact solution of ac electro-osmotic flow in a microannulus", *Journal of Fluids Engineering*, Vol. 135, No. 9, (2013), 91-100.
16. Moghadam, A.J., "Effect of periodic excitation on alternating current electroosmotic flow in a microannular channel", *European Journal of Mechanics-B/Fluids*, Vol. 48, (2014), 1-12.
17. Zhao, C. and Yang, C., "Electro-osmotic mobility of non-newtonian fluids", *Biomicrofluidics*, Vol. 5, No. 1, (2011), 211-221.
18. Zhao, C. and Yang, C., "Electroosmotic flows of non-newtonian power-law fluids in a cylindrical microchannel", *Electrophoresis*, Vol. 34, No. 5, (2013), 662-667.
19. Tang, G., Li, X., He, Y. and Tao, W., "Electroosmotic flow of non-newtonian fluid in microchannels", *Journal of Non-Newtonian Fluid Mechanics*, Vol. 157, No. 1, (2009), 133-137.
20. Mondal, S. and De, S., "Effects of non-newtonian power law rheology on mass transport of a neutral solute for electroosmotic flow in a porous microtube", *Biomicrofluidics*, Vol. 7, No. 4, (2013), 185-194.
21. Chhabra, R. and Richardson, J., *Non newtonian flow and applied rheology*. 2008, Elsevier, Amsterdam.
22. Bird, R.B., Armstrong, R.C., Hassager, O. and Curtiss, C.F., "Dynamics of polymeric liquids, Wiley New York, Vol. 1, (1977).
23. Davis, M.E., "Numerical methods and modeling for chemical engineers, Courier Corporation, (2013).

## Time-periodic Electroosmotic Flow of Non-newtonian Fluids in Microchannels

A. Jabari Moghadam, P. Akbarzadeh

Department of Mechanical Engineering, Shahrood University of Technology, Shahrood, Iran

P A P E R I N F O

چکیده

### Paper history:

Received 12 December 2015

Received in revised form 02 January 2016

Accepted 03 May 2016

### Keywords:

Microfluidics

AC Electroosmotic Flow

Shear-thinning and Shear-thickening Fluids

Circular Microchannel

Frequency

جریان الکترواسموتیک متناوب سیال غیرنیوتنی پاورلا در میکروکانال گرد مورد مطالعه قرار گرفته است. برای حل معادلات غیرخطی پواسون-بولتزمن و مومتوم، یک روش عددی به خدمت گرفته شده است. پارامترهای اصلی موثر بر میدان جریان عبارتند از: شاخص رفتار جریان، پتانسیل زتای بدون بعد و فرکانس بدون بعد. در فرکانس‌های بدون بعد خیلی کوچک (حرکت نوسانی کند، اندازه کانال کوچک یا ویسکوزیته موثر بزرگ) و تقریباً در تمام لحظه‌ها، پروفیل‌های سرعت توپی شکل شبیه به جریان الکترواسموتیک حالت پایدار مشاهده می‌شوند. در فرکانس‌های بدون بعد خیلی بزرگ، می‌توان دید که جریان به ناحیه باریکی نزدیک دیوار کانال محدود می‌شود، درحالی‌که سیال بالک ساکن باقی می‌ماند. در مقادیر کم فرکانس بدون بعد، توزیع سرعت مربوط به سیالات شبه پلاستیک و دیلاتانت ممکن است به صورت گسترده باشد که به پتانسیل زتای بدون بعد بستگی دارد؛ اما در فرکانس‌های بدون بعد زیاد، هر دو نوع این سیالات، مقدار سرعت افزایشی را نسبت به پتانسیل زتای بدون بعد نمایش می‌دهند. در حالت نرخ برش زیاد و یا آغاز ناگهانی جریان، شبه پلاستیک‌ها سرعت‌های بیشتری را نسبت به دیلاتانت‌ها تولید می‌کنند. این دو نوع سیال می‌توانند پروفیل‌های سرعت یکسانی ایجاد کنند که به مقدار پتانسیل زتای بدون بعد و نیز نسبت شاخص رفتاری آنها وابسته است.

doi: 10.5829/idosi.ije.2016.29.05b.15